Development of Advanced Solutions for Assessing the HFRW Technology in Green Energy Initiatives

M. Sadeghi [1,*], H. Sabet[2,3]

[1]*Department of Materials Technology Center, Perth, Western Australia.*
[2] *Department of Materials Engineering, Ka.C., Islamic Azad University, Karaj, Iran.*
[3] *Institute of Manufacturing Engineering and Industrial Technologies, Ka.C., Islamic Azad University, Karaj, Iran.*
Received: 09 April 2025 - Accepted: 17 September 2025

Abstract

In this article, the development of advanced solutions for assessing the HFRW technology in green energy initiatives has been studied. HFRW was implemented on actual samples by changing multiple parameters, including electric potential, current of welding, travel speed, and fin pitch. Meanwhile, metallography of the weld bond, tensile strength, and hardness tests were performed on several sections of the samples according to international standards for finned tubes. The diffusion zone, indicating the schematic of weld width and weld depth of the finned tube, is observed under the scanning electron microscope (SEM), which is used for analyses of melting and weld depth determination. The requirements, or the acceptance criteria of weld width, are that the weld width must be ≥ 90% of fin thickness, which can be calculated at the weld interface, with the application of optimum welding parameters. Moreover, as the pitch and fin thickness are reduced, the output transfer surface treatment in the final process diminishes. Hence, the parametric optimization of HFRW and the higher quality of the finned tube welding bond are revealed by the best conditions of fin pitch.

Keywords: Finned Tube, High-Frequency, Resistance Welding.

1. Introduction

Finned tube headers are routinely used in high-temperature applications in which heat recovery steam generators (HRSGs) are an integral part of any modern combined cycle power plant (CCPP). These heat exchangers are designed to recover the heat from a gas turbine exhaust and convert this to steam, which drives a turbine and ultimately a second generator. Because the gas turbine operates efficiently at high temperatures and heat is removed down to nearly ambient temperature, it increases flexibility and response to load dispatch. HRSG can be complex to analyse and also difficult to effectively test and prove their performance [1,2].

Fig. 1. A block of a combined cycle power plant (CCPP).

The current development in the power generation industry is of increasing demand for combined cycles with improved efficiency and reduced delivery time. Improved efficiency reduces the fuel-related cost and, at the same time, contributes to the resolution of the greenhouse effect. The finned tubes' position of harp modules in HRSG are key components in the combined cycle [2].A block of a combined cycle power plant (CCPP) is demonstrated in Fig. 1.

The surface area on the outside of the tubes is extended by finning in order to increase the rate of heat exchange in the heat recovery steam generator (HRSG) tubes [3]. In the finned tube welding process rolled steel strip is continuously welded in spiral form on the outside diameter of a tube. This type of weld is comprised of a fusion between two portions of parent metal without the introduction of a filler material. The weld is simply produced by heating the interfaces to be joined to a plastic state and applying pressure. The current frequency range normally used for high-frequency welding is 400 kHz. [4].

Fig. 2. HFRW technologies for making finned tubes.

Spiral finned tubes are now widely used in electricity, metallurgy, the cement industry, waste heat recovery,

[*]*Corresponding author*
Email address: Sadeghi.m2024@gmail.com

and petrochemical industries. Finned tubes, is to improve the efficiency of heat transfer, usually in the surface of the heat transfer tubes by adding fins, increasing heat transfer tube outer surface area (or internal surface area), so as to improve heat transfer efficiency purposes, such a change heat pipe. Finned tubes with continuous rib or serrated, depending on the operating parameters of the working medium and the flue gas, can be used as heaters, economizers or superheaters [5]. HFRW technologies for making finned tubes are demonstrated at Fig. 2.

Kocurek and Adamiec. studied that there are several technologies for making finned tubes. As a result, they are a suitable candidate for using and so that one of the most efficient welding processes of dissimilar metals and alloys is laser welding technology [6]. Adamiec and Więcek. mentioned that laser-welded joints of fin tubes made of alloy Inconel 625 are resistant to electrochemical and pitting corrosion in the base material [7].

Erling reported that high-frequency welding is a solid resistance heat energy. The use of high-frequency current welding resistance heat generated within the workpiece so that the workpiece surface is heated to melt the weld zone or close to a plastic state, then applied (or not applied) upsetting force to achieve binding metal [8]. Mcilwain. explained that it is a solid-phase resistance welding method, with this technique, the fin is wound on edge around the tube spirally, and a continuous weld is obtained [9]. The high-frequency resistance welding process produces a strong metallurgical bond between the fin and the tube while minimizing the heat-affected zone (HAZ) in the tube, as stated by Noordermeer and Eng. [10]. Huseman. investigated that the fins greatly enhance the heat transfer surfaces, allowing the full optimization of heating surfaces of the boiler, which is achieved by reducing the dimensions of the boiler, and thus reducing its weight [11]. As shown in Kushima et al. [12] a metallographic atlas for 2 .25 Cr-1Mo steels and degradation due to long-term service at elevated temperatures. King [13] performed that welding 2.25 Cr-1Mo steel is to use preheat and post-welding heat treatment (PWHT) to improve weldability. Wagner Ferreira et al. [14] indicated that microstructure evolution and creep properties of 2.25 Cr-1Mo ferrite-pearlite and ferrite-bainite steels after exposure to elevated temperatures. The observations of the ferrite-bainite steel show a more stable behaviour at the ageing temperatures and time considered. However, creep tests revealed that the ferrite-pearlite microstructure possesses a better rupture time performance. Zuback et al. [15] demonstrated that dissimilar joints between 2.25 Cr-1Mo steel to austenitic alloy (800H) show that eliminate abrupt changes in mechanical properties, microstructure, and composition with reduced carbon potential gradient. Ornek [16] observed the position of AISI 409, finned the lowest chromium content of all stainless steels in the Schaeffler diagram.

2. Materials and Methods

The chemical composition of AISI 409 is titanium-stabilised ferritic stainless steel (FSS) cold-rolled coil strips containing about 11% chromium, shown in the Table. 1. (according to ASTM A240). The presence of Cr leads to the formation of a passive surface film, which provides corrosion resistance. The addition of Ti prevents the formation of harmful Cr carbides, which can lead to intergranular corrosion in service. Type 409 is very similar to carbon steel, but 409 offers improved corrosion resistance in comparison to carbon steel. Ferritic stainless steels suffer embrittlement on welding due to grain growth and grain boundary martensite formation in the heat-affected zone that is heated above 1100°C. Preheating to 200°C and post-heat treatment at 750–850°C are recommended.

Table. 2. presents the chemical composition of the SA213-T22 (2.25 Cr-1Mo) material used in this study by an optical emission spectrometer, along with the ASTM A213-T22 compositional tolerances. High-pressure T22 has seamless steel for boiler, superheater, and heat exchanger tubes. The standard actually covers 14 different grades of ferritic steels and 14 different grades of austenitic steels. The addition of Cr to this alloy provides oxidation resistance and microstructural stability. Cr forms carbides within the grains that anchor the structure at high temperatures. Cr additions also significantly increase the hardenability of the alloy, thus increasing as-welded strength. The purpose of Mo in the alloy is to increase creep strength.

Table. 1. Chemical composition (%wt.) of the studied FSS fined and ASTM A240TP409 specification.

Steel Finned	C	Mn	P	S	Si	Cr	Ni	Ti
AISI 409 FSS	0.060	0.290	0.020	0.015	0.570	11.140	0.140	0.190
ASTM A240TP409	0.080	1.000	0.045	0.045	1.000	10.500-11.750	0.500	$0.500_{(max)}$

Table. 2. Chemical composition (%wt.) of the studied T22 (2.25 Cr-1Mo) tube and ASTM A213T22 specification.

Steel Tube	C	Mn	P	S	Si	Cr	Mo
T22 (2.25 Cr-1Mo)	0.120	0.400	0.013	0.003	0.230	2.150	0.930
ASTM A213T22	0.050-0.150	0.300-0.600	$0.025_{(max)}$	$0.025_{(max)}$	0.500-1.000	1.900-2.600	0.870-1.130

Table. 3. HFRW Welding parameters of sample test.

Sample No.	A213T22 tube Outside diameter × Thickness	AISI 409 finned Width× Thickness	Travel Speed (RPM)	Potential, Welding (V)	Current, Electric (A)	Pitch (Fins/Meter)
1	38.1×4.4	17×1.2	580	10.9	12.8	126
2	38.1×4.4	17×1.0	550	10.7	12.4	126
3	38.1×4.4	17×1.2	530	11.3	13.5	180
4	38.1×4.4	17×1.0	530	11.1	13.1	180
5	38.1×4.4	17×1.2	510	11.6	14.0	240
6	38.1×4.4	17×1.0	510	11.5	14.2	240
7	38.1×4.4	17×1.2	475	11.7	14.3	276
8	38.1×4.4	17×1.0	475	11.8	14.4	276
9	38.1×4.4	17×1.2	430	12.1	14.5	305
10	38.1×4.4	17×1.0	460	12.3	15.1	305

Serrated finned tubes and solid finned tubes are two types of spirals wrapped finned tubes used in HF, as illustrated in Fig. 3.

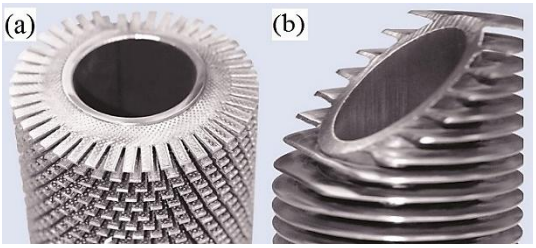

Fig. 3. Type of finned tubes HFRW process. (a) Serrated finned tubes, (b) Solid finned tubes.

Solid and serrated fins are widely used solutions for improving heat transfer in fired heaters. The important fact that designers often overlook while selecting the fins is that serrated fins can provide a larger surface area and significantly higher fin efficiency compared with solid fins.

Sample preparation of finned tubes welding metallography includes sample of weld bond tests, tensile strength and hardness tests were prepared as illustrated in (Fig. 4).

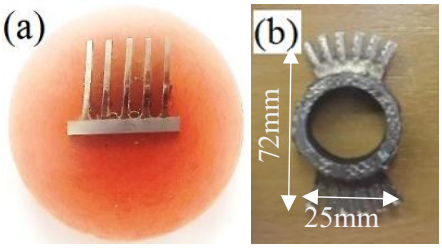

Fig. 4. Sample tests preparation of AISI 409 st-st to T22 boiler tube (a) metallography and hardness (b) tensile strength.

In this research, 4 essential welding parameters, including current, electric potential, welding speed (rotation speed) and pitch, were assumed as variables and 10 simples were selected by the Taguchi method and the welding process was performed according to the conditions mentioned in the Table. 3. by the "HANSUNG HFS-9488pu" HFRW machine.

After the welding process, sampling was performed according to international standards for tests of high-frequency resistance-welded fins based on ASTM E3 and ASTM E340. Metallography for the welding bond was done by an Olympus DMI3000M optical microscope, which was equipped with an image analyzer. The dimensions of the 2.25Cr-1Mo steel tube for welding experiments, 38.1×4.4mm, were selected. According to ASTM E340-22, at least 8 sections were prepared for the welding bond of the metallography test. The microstructure of the joints is analyzed with respect to their welding bond value. A minimum of 90 % welding bond should be obtained for acceptance according to the standard specifications of the welding machine manufacturer. Fin to fin-to-tube penetration of the welding bond is illustrated in Fig. 5. The 90 % welding bond minimum criterion is for each tube-fin joint.

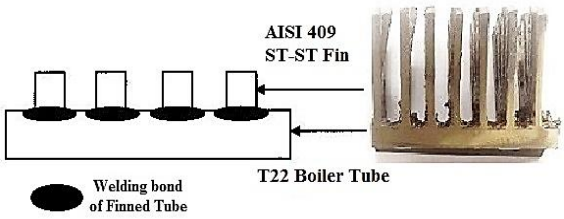

Fig. 5. Fin to tube penetration of the welding bond.

3. Results and Discussions

The microstructure of the ferritic grade of type 409 stainless steel finned is illustrated in Fig.6a. Recrystallized microstructure with an abundance of titanium carbides and carbonitrides. (Etch: 25 ml HN03, 25 ml acetic, 5 ml Hel, 50 ml glycerol) A straight chromium steel in which the carbon is deliberately kept as low as to have a negligible hardening effect is classified as ferritic. The chromium content is usually above 11 weight per cent with low carbon and no nickel; these alloys are permanently ferritic. It is shown the ferritic structure

with small grain size for the stainless steel 409. As well as the microstructure high pressure T22 boiler tube is shown in Fig.6.

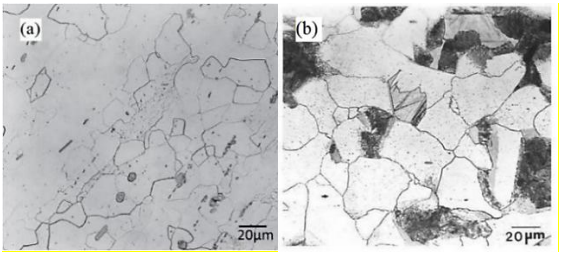

Fig. 6. The microstructure of (a) AISI 409 stainless steel (b) High-pressure T22 boiler tube.

The microstructure of typical 2.25 Cr-1Mo alloy steel tube consists of ferrite (light etching constituent) and a small amount of pearlite (dark etching constituent). Light tan areas are martensitic. It is interesting to note that if the same steel was used for a forging or plate, it may have a different microstructure because of the different specified heat treatment. ASTM A213 tubes can be furnished in the full-annealed, isothermally annealed, or normalized and tempered condition. Each condition would have a different microstructure.

The martensitic phase in this steel is due to the production method. According to continuous cooling transformation (CCT) diagram for 2.25Cr-1Mo steel is shown in Fig. 7. According to the Schaeffler diagram, in this case, the amount of chromium and nickel equivalent is displayed in Fig. 8. The examined sample steel had a ferrite type.

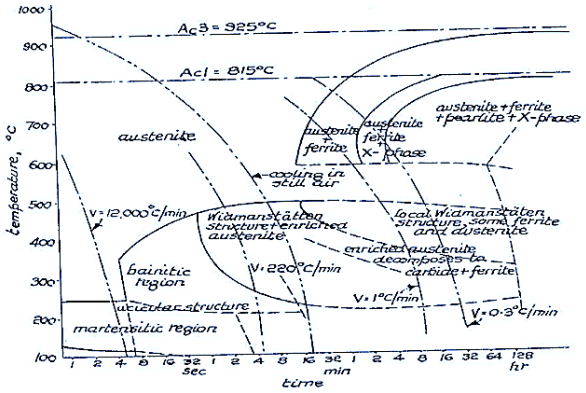

Fig. 7. CCT diagram of high-pressure T22 boiler tube.

A fin-to-tube joint showing a 100% welding bond is shown in Fig. 9.a. By contrast, a joint showing an incomplete 84% welding bond is shown in Fig.9. b. The welding bond should be at least 90 per cent according to the standard specification for high-frequency electric resistance welded finned tubes.

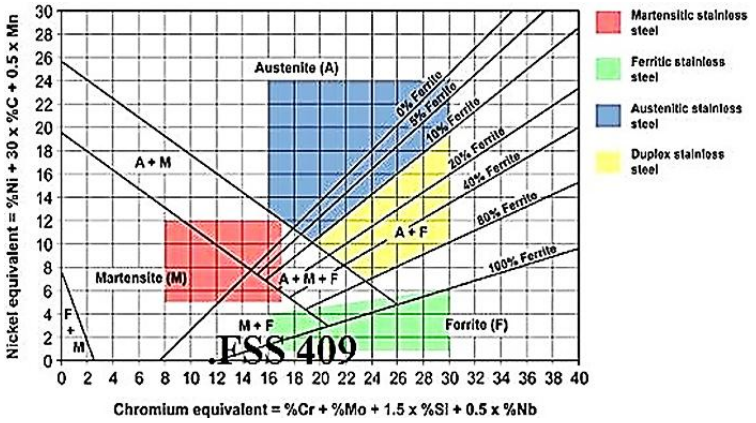

Fig. 8. The position of AISI 409 ferritic stainless steel (FSS) in Schaeffler diagram. [17]

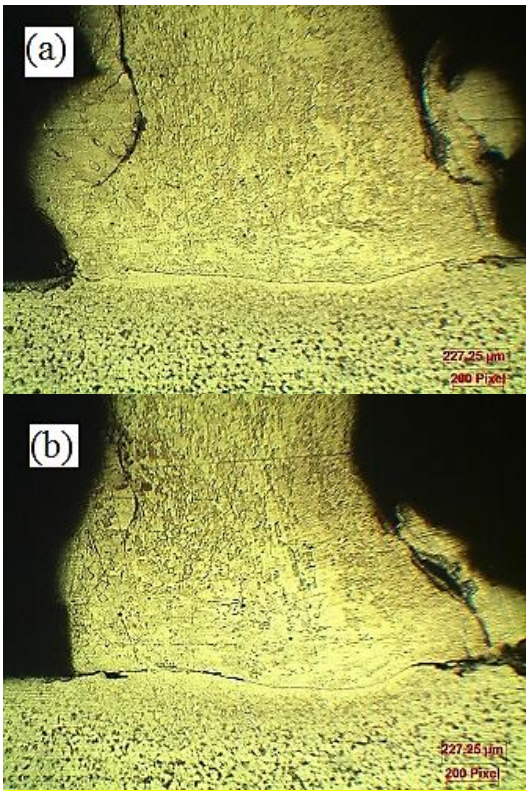

Fig. 9. The microstructer of AISI 409 FSS to T22 boiler tube (a) Accepted sample: 100% weld bond (b) Rejected sample: 84% weld bond.

Butt weld joint is quantitatively considering the specimen using the acceptance criteria (Q) by measuring S (weld width (mm)) and D (weld depth (mm)) values from the microstructure micrograph. The Fig.10. Shows the schematic of weld width and weld depth of finned tube observed under the scanning electron microscopy (SEM) which is used for analyses melting and weld depth determination. There requirements or the acceptance criteria of weld width are that the weld width must be ≥ 90% of fin thickness which can be calculated using equation (1)

and the weld depth must be in the range of 0.05 - 0.30 mm.

a) Weld width: Q = (S/T) x 100 (1)

When T = Nominal thickness of fin (mm)

S = Weld Width (mm)

Acceptance Criteria: Q ≥ Average 90% of nominal fin thickness

b) Weld Depth

Acceptance Criteria: 0.05 < D < 0.30 mm

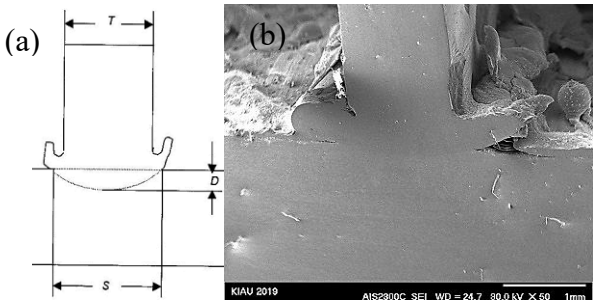

Fig. 10. (a)Schematic of weld width and weld depth of finned tube (b) the scanning electron microscopy (SEM).

At least 8 samples finned to tube were prepared, for welding bond test. As given in Table 4, obtained clearly more than 90% welding bond average quality for ten samples by applying optimum welding parameters, fin-tip and tube-tip position and setting on squeeze rollers with hydraulic pressure jack: a) Air pressure of fin tip holder is 0~4 kg/㎠, b) Air pressure of tube tip holder 0~5 kg/㎠, pitch or fin per meter (FPM).

Table. 4. Average of welding bond sample .

No.	Fin to tube weld bond	Result
1	100 %	Accept
2	100 %	Accept
3	95 %	Accept
4	100 %	Accept
5	97 %	Accept
6	99 %	Accept
7	100 %	Accept
8	100 %	Accept
9	100 %	Accept
10	100 %	Accept

Tensile strength curves of 6 fin joints to tube illustrated that Fig. 11a. rejected sample and Fig.11b. accepted sample No.8. As well as the result of tensile strength is displayed in Table 5.a rejected sample and Table. 5.b accepted sample No.8

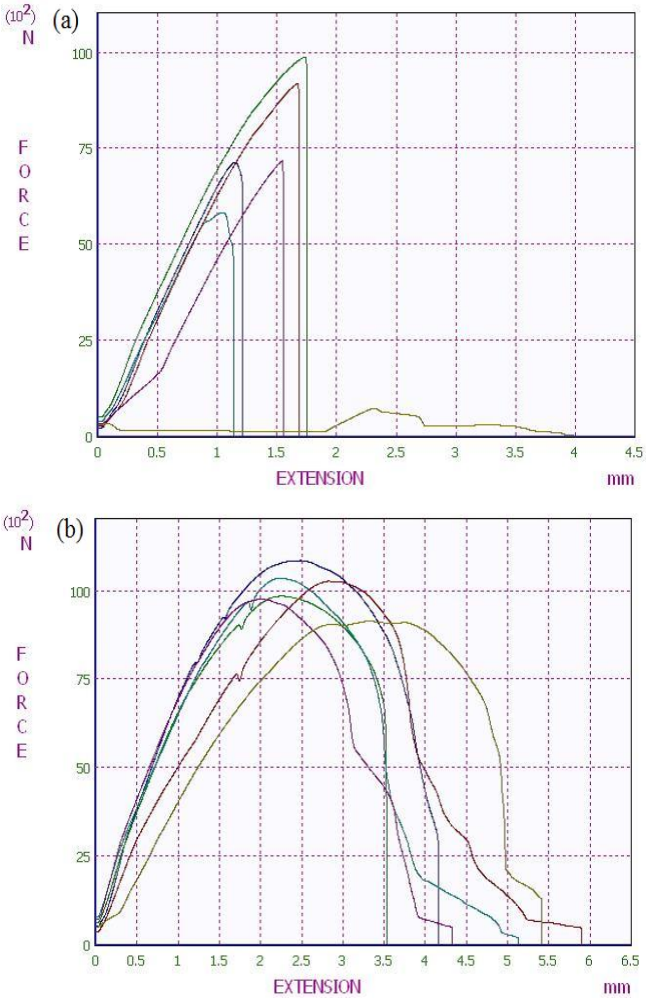

Fig. 11. Tensile strength of tube to fins according to ASTM A370-22 (a) rejected sample (b) accepted sample No.8.

The result of tensile strength in Table 5 indicate that the lowest ultimate tensile strength (UTS) was 324.58 MPa and the average of UTS in theses case was 341.76. Table. 6. shows result of average tensile strength for the 10 samples. Furthermore, all of the sample tests were accepted because the average of tensile strengths were more than 275MPa.

The results of hardness tests at four different places in the samples are given in Table 7, as well as the hardness variations. The position of hardness test (fin, tube and HAZ) is exhibited in Fig.12.

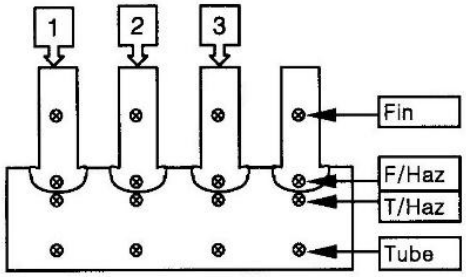

Fig. 12. Position of hardness test (fin, tube and HAZ)

Table. 5. Result of tensile strength (6 fin joint to tube) (a) rejected sample (b) accepted sample No.8.

(a)

Specimen	Thickness(mm)	Sec. Area (mm^2)	Total load (N)	UTS (MPa)	Location of failure
T1	1.2	29.244	7141.88	244.27	Weld
T2	1.2	25.428	9863.14	387.88	Weld
T3	1.2	27.756	5817.53	209.56	Weld
T4	1.2	26.364	9188.7	348..53	Weld
T5	1.2	26.592	7176.63	269.88	Weld
T6	1.2	27.492	726.55	26.43	Weld
Result	**REJECT**				

(b)

Specimen	Thickness(mm)	Sec. Area (mm^2)	Total load (N)	UTS (MPa)	Location of failure
T1	1.0	27.564	10847.2	393.53	Fin
T2	1.0	30.072	9841.68	327.270	Fin
T3	1.0	30.132	10347.51	343.40	Fin
T4	1.0	30.468	10262.69	336.83	Fin
T5	1.0	30.06	9747.67	324.92	Fin
T6	1.0	28.152	9137.61	324.58	Fin
Result	**ACCEPT**				

Table. 6. Average tensile strength of welding sample.

No.	Tensile strength (MPa)	Result
1	380.31	Accept
2	378.39	Accept
3	375.34	Accept
4	377.85	Accept
5	376.24	Accept
6	381.15	Accept
7	380.17	Accept
8	379.57	Accept
9	375.61	Accept
10	379.73	Accept

Table. 7. Hardness results of various sample (HV)

No.	Fin HAZ	Hardness variation of fin-to-fin HAZ	Tube HAZ	Hardness variation of tube-to-tube HAZ
1	174	151	252	168
2	162	165	270	166
3	165	156	263	163
4	170	149	249	166
5	166	160	264	164
6	171	150	267	167
7	169	148	265	163
8	160	162	273	164
9	172	159	262	161
10	164	161	258	162

Table. 8. Hardness result of rejected sample.

No.	Hardness (HV)			
	Fin HAZ	Hardness variation of fin-to-fin HAZ	Tube HAZ	Hardness variation of tube-to-tube HAZ
1	198	189	277	178

The highest hardness in HAZ alloy steel tube 273 HV was related to sample No.8 and the lowest hardness in alloy steel tube 249 HV was related to sample No.4. As well as the highest hardness in HAZ St-St finned, 174 HV was related to sample No. 1 and the lowest hardness in HAZ St-St finned, 160 HV related to sample No.8.The most hardness variation between HAZ fin to fin 165 HV related to sample No. 2 and the most hardness variation between HAZ tube to tube 168 HV related to sample No. 1. Cycle heat due to high cooling rate accompanied by water spray led to the grain size microscopic structure and HAZ limited in section welding so that the average of tensile strength was more than 275 MPa and all the hardness samples were in acceptance criteria according to ASTM E384-022 standard, as well as in Table. 8., one rejected sample was provided just to be compared with accepted samples.

We apply different specifications and acceptance criteria for solid fin tube types compared to serrated fin tubes. Serrated and solid types of fin tubes produced by HFRW depend on fin height, fin thickness, and tube O.D. The result of analyzes show that as the lower pitch and fin thickness are selected, the higher quality of fin tube welding bond is achieved. On the other hand, as the pitch and fin thickness is reduced, the output transfer surface treatment in final process decreases. So, for increasing performance in the aspect of process design and welding engineering, the current welding is set on optimum electric potential, and it depends on the travel speed of welding. As well as selecting suitable finned obtained by over 15mm fin high, 1mm fin thickness and 276 per meter of fin pitch, the higher quality of finned tube welding bond is achieved.

4. Conclusion

In this research, development of advanced solutions for assessing the HFRW technology in green energy initiatives was investigated. The key findings are summarized below:

1. A diffusion zone indicating the weld width and weld depth of the finned tube was observed under SEM. For optimal bonding, the weld width must be at least 90% of the fin thickness, which can be calculated at the weld interface.
2. The optimization of welding parameters and squeeze roller settings demonstrated that high-quality metallurgical bonding of finned tubes is achieved under the most favorable fin pitch conditions.
3. Water spray cooling resulted in a refined grain structure and a confined heat-affected zone (HAZ). The average tensile strength exceeded 275 MPa, and all hardness test samples met the acceptance criteria.
4. Parametric optimization of HFRW for finned tube welding was successfully achieved. The optimal conditions were identified as a fin pitch of 276 fins per meter, fin height greater than 15 mm, and fin thickness of 1 mm.
5. The key factors influencing the HFRW process are fin height, fin thickness, and tube outer diameter (O.D.), applicable to both solid and serrated types of spiral finned tubes.

References

[1] Sadeghi M, Sabet H. Energy saving technology in power plants industry by high frequency resistance welding. Paliva. 2022;14(3):117–123.
[2] Benton DJ. Heat Recovery Steam Generators: Thermal Design & Testing. Independently Published. 2019.
[3] Wang Y, Adumene S. Heat Recovery Steam Generator Technology. Scitus Academics LLC. 2019.
[4] Eriksen V. Heat Recovery Steam Generator Technology. Woodhead Publishing. 2017.
[5] Dziemidowicz Z, Szyszka P, Krupa I. Power units on the horizon: technical requirements of new generation units at PGE Power Plant Opole S.A. Electric Heat and Vocational Education.2011;11:14-20
[6] Pis'mennyi E, Georgiy P, Ignacio C, Florencio S, Pioro I. Handbook for Transversely Finned Tube Heat Exchanger Design. Academic Press. 2016.
[7] Kocurek R, Adamiec J. Manufacturing technologies of finned tubes. Advan in Mat Sci. 2013;13(3):29-35.
[8] Adamiec J, Więcek M. Technology for laser welding of ribbed pipes made of Inconel 625 nickel alloy. Biuletyn Institute Spawalnictwa. 2014;5:40-49.
[9] Erling N. Experimental investigation of heat transfer and pressure drop in serrated-fin tube. App Ther Eng. 2010;1534:20-28.
[10] McIlwain SR. A comparison of heat transfer around a single serrated. IJRRAS. 2010;2:88-93.
[11] Noordermeer J, Eng P. Introduction to gas turbine, cogeneration and combined cycle application. IAGT Symposium Training Sessions. Banff, Alberta. 2013: 85–94.
[12] Huseman R. Advanced (700°C) PF power plant: A clean coal European technology. Advanced Material for AD700 Boilers. Cesi Auditorium, Milano. 2010: 93-105.
[13] Kushima H, Watanabe T, Murata M, Kamihira K, Tanaka H, Kimura K. Metallographic atlas for 2.25Cr–1Mo steels and degradation due to long-term service at elevated temperatures, ECCC Creep Conf. 2005; 223–239.
[14] King B. Welding and Post Weld Heat Treatment of 2.25%Cr–1%Mo Steel [Master's thesis]. University of Wollongong. 2005.
[15] Ferreira LW, Glaucio R, Heloisa C, Furtado M, Barreto L, Luiz Henrique de A. Microstructure evolution and creep properties of 2.25Cr–1Mo ferrite-pearlite and ferrite-bainite steels after

exposure to elevated temperatures. Mate Rese.2017;10(1):590–601.
[16] Zuback S, Mukherjee T, Palmer TA, DebRoy T. Novel dissimilar joints between 2.25Cr–1Mo steel and Alloy 800H through additive manufacturing. AWS FABTECH Conference. Las Vegas. 2016; 121–129.
[17] Ornek C. Performance Characterisation of Duplex Stainless Steel in Nuclear Waste Storage Environment [PhD thesis]. University of Manchester. 2015.
[18] Guiraldenq P, Duparc OH. The genesis of the Schaeffler diagram in the history of stainless steel. Metall Res Technol. 2017; 114:613-622
[19] ASTM International. ASTM A240: Standard Specification for Heat-Resisting Chromium and Chromium-Nickel Stainless Steel Strip for Pressure Vessels. 2022.
[20] ASTM International. ASTM A213: Standard Specification for Seamless Ferritic and Austenitic Alloy-Steel Boiler, Superheater, and Heat-Exchanger Tubes. 2022.